Frontiers in Scientific Research and Technology

Online ISSN: 2682-297
Print ISSN: 2682-2962
http://fsrt.journals.ekb.eg

FSRT J 4 (2022) 33 - 38 10.21608/fsrt.2022.136873.1063

Tracking of the development of a vortex ring in isotropic turbulence

Waleed Abdel Kareem*, Hadeer Mohammed, Zafer Asker, and Hamed El Sherbiny

Department of Mathematics and Computer Science, Faculty of Science, Suez University, Suez, Egypt

ARTICLE INFO

Article history:
Received 4 May 2022
Received in revised form 26 May 2022
Accepted 27 May 2022
Available online 28 May 2022

Keywords
Isotropic turbulence;
Vortex ring;
Vortex tracking;
LBM;
D3Q19

ABSTRACT

In the current study, the isotropic turbulence, and the lattice Boltzmann method (LBM) are utilized as helpful tools to track the development of a vortex ring in isotropic turbulence. A vortex ring is isolated from a decaying turbulent flow with a resolution of 128^3, and three different approaches are considered to deal with the single vortex ring. The first case has started at null velocity, considering the vortex ring as a forcing source where the velocity modes at low wavenumbers are calculated using the stored vorticity data from the Poisson equation $\vec{\nabla} \times \vec{w} = -\nabla^2 \vec{u}$ in the Fourier space. Then, large tubular vortices are found, and the ring has broken as a result of being an external force every time step. In the second case, the vortex ring is used as an initial state and left to dissipate, and large tubular vortices are formed around the ring due to the presence of a tube source. Finally, an initial state from a forced turbulent flow is used, and the vortex ring is also utilized as a forcing source every time step in the LBM. The vortex ring has broken and interacted with the tubular vortices from the forced turbulence forming a variety of thin tubular vortices. The three cases are studied and compared, moreover, some statistical features of the flow field are calculated such as the Taylor-Reynolds number R_λ, the Taylor micro-scale λ, the Kolmogorov micro-scale η, and the energy spectrum function $E(k)$. It's found that the third case gives the best result, as the thin tubular vortices are conformed from the interaction of vortex tubes of the forced turbulence with the large ring in comparison to other cases. Also, the energy spectrum is developed for the third case and has the greatest $k_{max}\,\eta$ value among the three cases.

1. Introduction

Isotropic turbulence is a standard model of turbulence that mimics being far away from boundaries, as it's specified to be invariant under rotations and transitions. It is of two types, either forced or decaying [1,2,3]. Connected re-gions in turbulent flows with high vorticity values in which the flow revolves around an imaginary axis line are known as vortices, which are a major component of turbulent flows. They are also of two types, either free or forced with definite shapes such as tubes (worm-like), rings, hairpins, etc. In this paper, we are interested in the ring-like vortices (toroidal vortices) or simply the vortex rings. The region where the fluid spins around a hypothetical axis line but forms a closed loop is what we call a vortex ring, or in other words, it's the bounded region of vorticity in a fluid in which vortex lines form closed loops [4]. Vor-tex rings are plentiful in nature, they're mostly seen in the smoke ring when the cigarette smoke is suddenly ejected. Other examples contain microbursts [5], the mushroom-shaped cloud formed during an explosion, and artillery.

* Corresponding authors at Suez University

E-mail addresses: waleed.abdelkareem@sci.suezuni.edu.eg (Waleed Abdel Kareem)

They also exist in a wide variety of systems, such as in the human heart [6], turbulent gases [7], electromagnetic discharges [8], and in a bulk magnet [9]. Furthermore, vortex rings are found around the main rotor of helicopters causing a very dangerous aerodynamic condition known as vortex ring state (VRS) [10,11,12]. The vortex ring state is characterized by turbulent flow fields around the rotor in descending flights which cause significant loss of rotor control. This case was described briefly by Basset et al (2008) [13] as: "A helicopter rotor in descending flight may encounter its own wake resulting in a doughnut-shaped ring around the rotor disk, known as the vortex ring state".

Vortex rings can be generated in laboratories by vari-ous methods. For example, they can be generated through impulsively started jets with the aid of a piston/cylinder arrangement in a water tank [14], by a piston moving in-side a cylinder with a stroke length of two piston diame-ters [15], through shrouded Hartmann–Sprenger tube [16], or by using helium as driver gas [17].

Owing to the presence of vortex rings in nature, the formation and behavior of the vortex ring have impressed researchers over years. Starting from 1858, a vital year regarding vortex rings, Rogers [18] made sounding observations of the formation process of air rings in the air, air rings in liquids, and liquid rings in liquids. In this research, while studying the air-jets phenomena, a critical

examination of the conditions under which vortex rings discharge was produced, also, the tracking of the development of the rings was achieved, as well as forming similarly constituted rings from water and other liquids. Also, Helmholtz [19] analyzed vortex rings mathematically. Since then till now various attempts were made, Buzukov (1971) [20] investigated the properties of the formation and motion of vortex rings in water, and showed experimentally that after a vortex ring travels a specified distance, it becomes difficult to be distinguished. The final results were compared with the available theoretical data. Boyarintsev et al (1982) [21] studied the propagation of vortex rings in stratified fluids theoretically and experimentally. Pismen and Nepomnyashchy (1993) [22] studied the stability of an isolated vortex ring using the nonlocal equation of motion in the framework of the Ginzburg-Landau model. Instability was shown due to the nonlocal effect in the long scale. Orlandi and Verzicco (1993) [23] made three-dimensional numerical simulations on vortex rings impinging on walls which led to a good agreement with experimental studies. Tamano et al (2010) [24] performed flow visualization of vortex rings in confined swirling flow of polymer solutions due to a partially rotating disc.

A relation was created between the lower-critical Reynolds number for the vortex ring and the elastic number. Abdel Kareem (2011) [25] carried out direct numerical simulations of three-dimensional decaying isotropic turbulence with a resolution of 128^3. In his research, some vortical structures were tracked in a forward and backward manner. Moreover, a vortex ring was identified in the flow field which led to a good conclusion that vortex rings may exist in isotropic homogenous turbulence contrary to the usual. Murugan and De (2012) [26] carried out a numerical visualization of counter-rotating vortex ring formation at the open end of a shock tube at high-shock Mach number. Aydemir et al (2012) [27] investigated the formation of vortex rings in the developing region in a forced round jet. Harmonic velocity oscillations were achieved at several forcing frequencies. The time-resolved history of the formation process and circulation of the vortex rings was evaluated in terms of the forcing conditions.

Imamura and Matsuuchi (2013) [28] introduced a relationship between vortex ring formation in the wake of a tail fin in dolphins and fish and the propulsive force where the propulsive forces arising from vortex ring formation were calculated. They also showed that the three-dimensional structures of vortex rings based on two-dimensional data don't describe the characteristics of vortex rings correctly. The effect of piston velocity on the formation number of vortex rings was studied by Peng (2015) [29]. It was asserted that piston acceleration can delay the vortex ring pinch-off and the formation of secondary vortices. Tinaikar et al (2018) [30] investigated the evolution of vortex rings in viscous fluids. It was observed that both Saffman's thin-core model and the thick-core equations couldn't explain the vortex evolution for all initial conditions. While Bentata et al (2018) [31] carried out experimental studies of low inertia vortex rings in shear-thinning fluids at low generalized Reynolds numbers. The results showed independency of the vortex ring subsequent evolution on the power-law index. Rebah (2020) [32] proved the existence of steady vortex rings of an ideal fluid in a uniform flow. Yeo et al (2020) [33] studied the flow transition and vortical developments during vortex ring collisions with a sharp water-oil density interface. The results asserted that the vortex ring deformation of the density interface depends basically upon the Reynolds number.

In this paper, the development of a vortex ring in isotropic turbulence is tracked using the D3Q19 lattice Boltzmann model in three different cases. The three cases are investigated and compared to each other, and the results are visualized. The rest of the paper is organized as follows:

Sec.2 introduces the lattice Boltzmann method, sec.3 is devoted to the tracking procedure, while sec.4 represents the vortex visualization and discussion. Sec.5 is for the statistical features of the flow field. Finally, sec.6 represents the conclusion of the paper.

2. The Lattice Boltzmann Method

The lattice Boltzmann method is a relatively new method that's used for turbulent flow simulations. It became a promising alternative to the conventional Navier-Stokes equations as it's quite simpler and efficient.

Yu et al (2005) [34] utilized the decaying homogeneous isotropic turbulence to prove the efficiency of the LBM as a computational tool to perform direct numerical simulations (DNS) and large eddy simulations (LES) of turbulent flows. Also, Haussmann et al (2019) [3] investigated the stability and accuracy of various lattice Boltzmann schemes by applying numerical experiments on decaying homogeneous isotropic turbulence.

The Lattice Boltzmann method is based on the Boltzmann equation, which can be written in the lattice form as:

$$f_i(\vec{r}+\vec{e}_i\delta t, t+\delta t) - f_i(\vec{r},t) = -\frac{1}{\tau}\left(f_i(\vec{r},t) - f_i^{eq}(\vec{r},t) + \delta t\, f_i\right) \quad (1)$$

Where $f_i(r,t)$ is the probability of finding a particle at position r and time t with velocity $v = e_i$. The subscript i labels a set of discrete speeds connecting the nodes of a regular lattice, While τ is the relaxation time, and $\delta t\, f_i$ represents the forcing term [35]that can be added to the lattice Boltzmann equation by two methods, either by adding it to the collision term or by shifting the velocity field using Newton's second law to cause some disturbance in the turbulent flow. In this study, we made velocity shifting by using the velocities of the extracted vortex ring. f_i^{eq} is the local distribution function at equilibrium state that's written as:

$$f_i^{eq}(\vec{r},t) = w_i\rho\left[1 + 3(\vec{e}_i.\vec{u}) + \frac{9}{2}(\vec{e}_i.\vec{u})^2 - \frac{3}{2}(\vec{u}.\vec{u})\right] \quad (2)$$

Where ρ and $\vec{u}$ represent the fluid mass denisty and velocity. The weighting coefficients w_i for the D3Q19-model are:

$$w_i = \begin{cases} \frac{1}{3}, & i=0 \\ \frac{1}{18}, & i = 1-6 \\ \frac{1}{36}, & i = 7-18 \end{cases} \quad (3)$$

And, the discrete velocity set e_i for the D3Q19-model is defined as:

$$e_i = \begin{cases} (0,0,0), & i=0 \\ (\pm1,0,0),(0,\pm1,0),(0,0,\pm1), & i = 1-6 \\ (\pm1,\pm1,0),(\pm1,0,\pm1),(0,\pm1,\pm1), & i = 7-18 \end{cases} \quad (4)$$

3. Tracking Procedure

Simulations of a decaying isotropic turbulence with a resolution of 128^3 were carried out in a previous study by Abdel Kareem (2011) [25] where a vortex ring was identified. This vortex is extracted and then tracked in three cases as follows:

Case (1):

Starting at zero velocity, the vortex ring is considered as a forcing source in the lattice Boltzmann method and injected every time-step using the Poisson equation $\vec{\nabla} \times \vec{w} = -\nabla^2\vec{u}$ which is derived from the vorticity equation $\vec{w} = \vec{\nabla} \times \vec{u}$. The Poisson equation is solved in the Fourier space using the fast Fourier transform (FFT) to obtain the velocities, then the velocities are projected back to the physical space to be inserted in the lattice Boltzmann equation.

Case (2):

The vortex ring is used as an initial state and left to dissipate without additional forces.

Case (3)

An initial state from a forced turbulent flow that was simulated in a previous study by Abdel Kareem and Asker [2] is used, and the vortex ring is also utilized as a forcing source every time step in the lattice Boltzmann method.

The initial state of the forced turbulent flow is shown in Fg. 1.

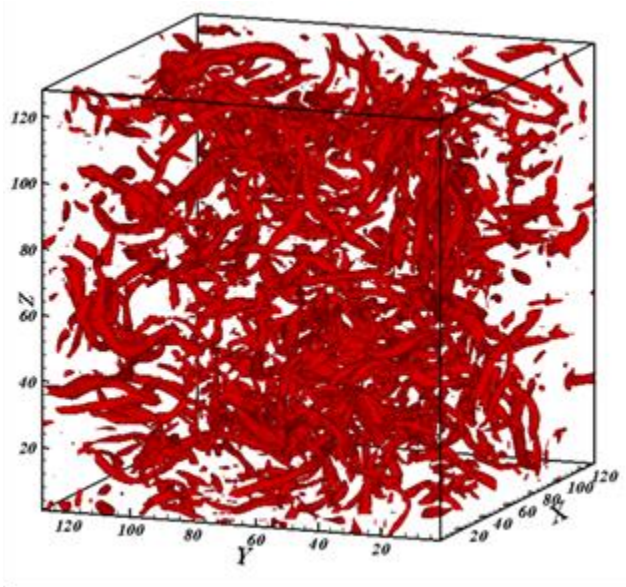

Fig. 1. Initial state: forced isotropic turbulence with resolution of 128^3

4. Discussion

4.1 Visualization of the vortical structures

The current subsection introduces visualizations of the tracking process for all the three cases. All vortical structures are visualized using the Q_s^s identification method [36] whose definition is:

$$Q_s^s = \left[(Q_w^3 + Q_s^3) + \left(\sum{}^2 - R_3^2\right)\right]^{\frac{1}{3}} \quad (5)$$

Here, Q_s represents the strength of the deformation rate, while Q_w represents the strength of the rotation rate. R_s is the strain rate production, and $\sum$ is the enstrophy production term. They are defined as:

$$Q_s = -\frac{1}{2}S_{ij}S_{ij}, \quad Q_w = \frac{1}{2}\Omega_{ij}\Omega_{ij} \quad (6)$$

$$R_s = -\frac{1}{3}S_{ij}S_{jk}S_{ki}, \sum = w_iS_{ij}w_j \quad (7)$$

Where $\Omega_{ij} = \frac{u_i,j-u_j,i}{2}$, $S_{ij} = \frac{u_i,j+u_j,i}{2}$ are the rotation and deformation tensors, and w_i is the vorticity vector.

Fig.2 represents the extracted vortex ring [25].. Fig.3 (a,b,c) introduces the tracking process for the first case at different time steps: *t=5, t=20,* and *t=50*. The tracking result shows formation of large tubular vortices, and the ring is broken as a result of being an external force every time step. Fig.4 (a,b,c) shows the tracking process for the second case at *t=5, t=20* and *t=50* where the vortex ring is used as an initial state and left to dissipates in the absence of a forcing source. By the time, large tubular vortices have formed around the ring due to the presence of a tube source. Fig.5 (a,b,c) represents the tracking process for the third case, where an initial state from a forced turbulent flow is used, and the vortex ring is also considered as a forcing source every time step in the LBM. The tracking result shows that the vortex ring has broken and interacted with the tubular vortices of the forced turbulence, forming variety of thin tubular vortices.

The third case gives the thinnest tubular vortices as the figure shows and as confirmed by the energy spectra in the following figure. Chen et al (2020) [37] performed a simulation of three-dimensional compressible decaying isotropic turbulence using a redesigned discrete unified gas kinetic scheme. The results of the third case are comparable to their simulation results of resolutions 256^3 and 512^3. The vortical structures are quite similar, but ours are thinner and more abundant, and the statistical features of the flow field are also very close.

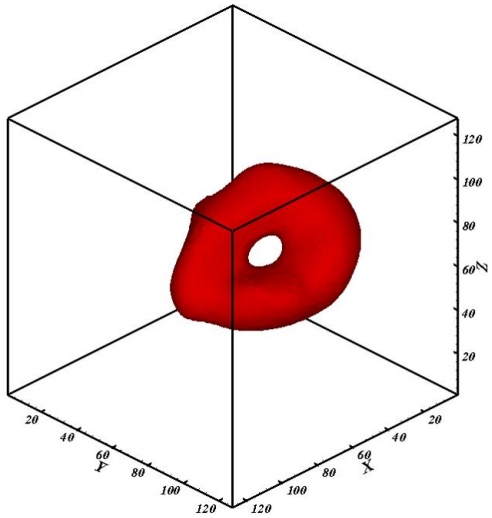

Fig. 2. The extracted vortex ring.

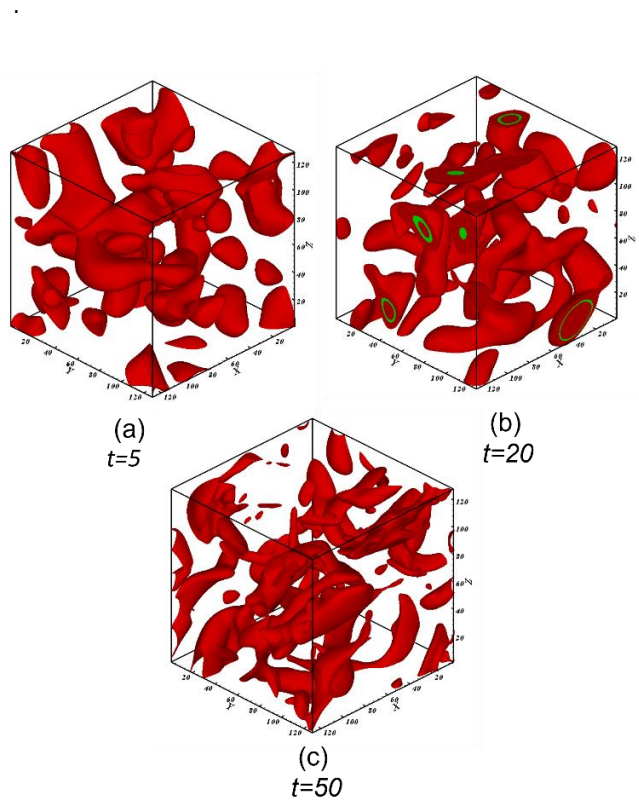

Fig. 3. Tracking process of the first case

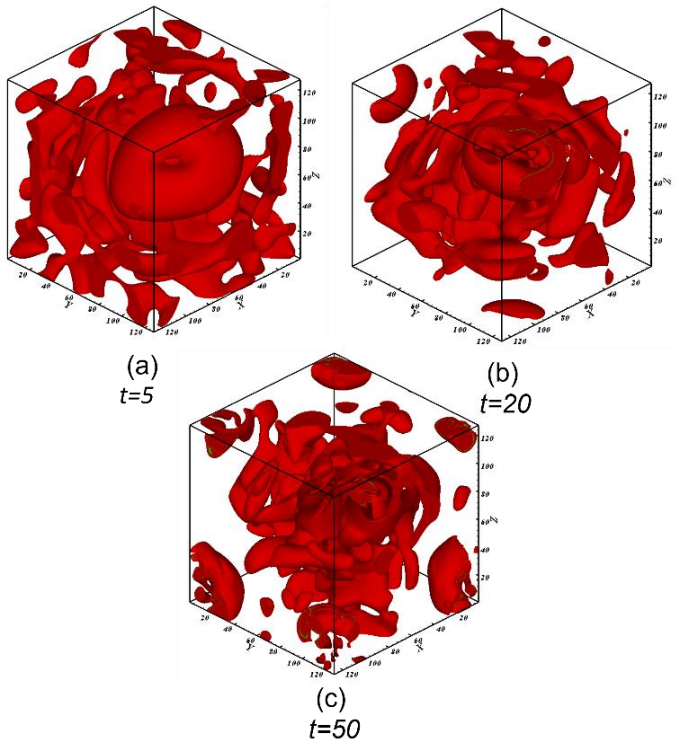

Fig. 4. Tracking process of the second case.

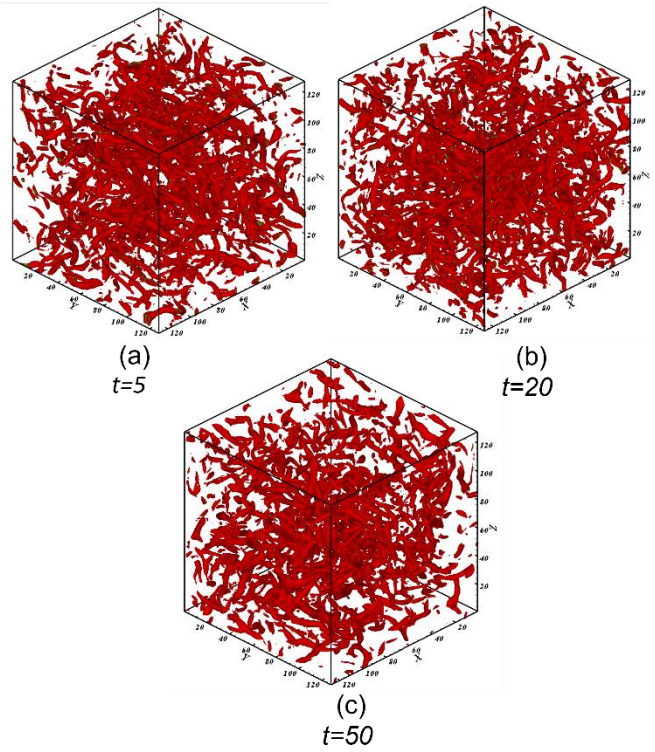

Fig. 5. Tracking process of the third case

4.2. Statistics of the energy spectrum

The spectrum function $E(k)$ in the spectral space at scalar wavenumber k is defined by:

$$E(k) = \frac{1}{2}\sum_{k-\frac{1}{2}<|k|\leq k+\frac{1}{2}} |\hat{u}^2(k)| \quad (8)$$

Where $\hat{u}$ are the velocity Fourier coefficients.

Fig.6 introduces the energy spectra for the three cases. At low wavenumbers, the energy spectrum for the first case has the greatest value which indicates having bigger vortices, unlike the third case which has the smallest value. At higher wavenumbers, we see that all the three cases have $k_{max}\,\eta > 1$ which is an indicator that they all contain thin vortices. But the energy spectrum of the third case has the greatest $k_{max}\,\eta$ value and the highest curve in comparison to the other cases, this means it developed the best, and it has the thinnest vortices due to the interaction with the tubular vortices of the forced isotropic turbulence.

.

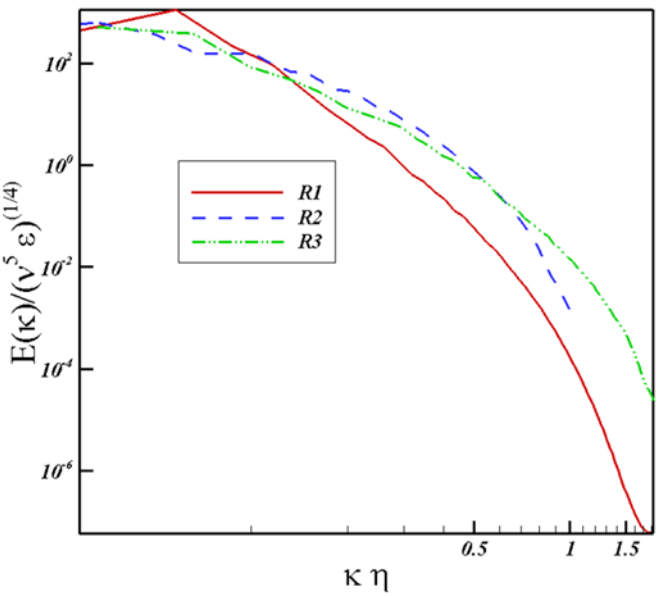

Fig. 6. Energy spectra for all cases

5. Validation of the numerical studies

Many features of the flow field such as the Taylor Reynolds number R_λ, Taylor micro-scale λ and the Kolmogorov micro-scale η can be used to characterize the homogeneous isotropic turbulent flow.

The Taylor Reynolds number is defined mathematically as:

$$R_\lambda = \frac{U_{rms}\lambda}{v} \quad (9)$$

Where U_{rms} is the root mean square (*rms*) of the velocity field.

$$U_{rms} = \frac{2}{3}\int_0^{k_{max}} E(k)\,dk \quad (10)$$

Here k_{max} is the maximum wavenumber whose definition depends on the resolution used in the simulation. The values of the Taylor-Reynolds number for decaying isotropic turbulence in direct numerical simulations (DNS) vary from 21 to 132 due to Wang et al [38], from 35 to 195 due to Sreenivasan et al [39], and from 0 to 2000 due to Bos et al [40].

The Taylor micro-scale:

$$\lambda = \sqrt{15U_{rms}^2/S_{ij}S_{ij}} \quad (11)$$

The Kolmogorov micro-scale η:

$$\eta = \left(\frac{\upsilon^3}{\varepsilon}\right)^{\frac{1}{4}} \quad (12)$$

Where ε is the average energy dissipation rate, and υ represents the viscosity.

The following table (1) summarizes the values of R_λ, λ, η and $k_{max}\,\eta$ for the three cases.

Table (1): Statistical characteristics of the flow field.

	R_λ	λ	η	$k_{max}\,\eta$
Case (1)	100.34	0.68	2.89×10^{-2}	1.82
Case (2)	94	0.63	1.65×10^{-2}	1.043
Case (3)	109	0.34	0.0327	2.058

6. Conclusion

A vortex ring was identified in a decaying isotropic turbulence with a resolution of 128^3 that was simulated in a previous study by Abdel Kareem [25]. Due to the previous literature, such vortex rings are rarely notable in isotropic turbulence because of the rapid interaction with the tubular vortices in the flow field. In this study, this vortex ring was extracted, and then tracked based on three approaches. It was treated firstly as a forcing source in the lattice Boltzmann method at null velocity and injected every time step. In a second attempt, the vortex ring was used as an initial state and left to dissipate where no additional force was considered. Finally, a forced isotropic turbulence was used as an initial state and the ring was considered as a forcing source. Due to the tracking processes, the third case gave the thinnest vortices among the three cases as the vortex ring interacted with the tubular vortices of the forced turbulence producing a large variety of tubular vortices. In this case, the initial state affected the ring causing rapid vortex breaking and giving thinner vortices.

Acknowledgment

This paper is based upon work supported by Science, Technology & Innovation Funding Authority (STDF)-Egypt under grant No. (25865).

References

[1] W. Abdel Kareem, Z. Asker, H. Mohammed, and H. El Sherbiny“, Lattice Boltzmann high performance simulations of decaying isotropic turbulence”, submitted February, 11th, 2022.

[2] W. Abdel Kareem, and Z. Asker, “Simulations of isotropic turbulent flows using lattice Boltzmann method with different forcing functions”, International journal of modern Physics C (2022), 2250145(24pages).

[3] M. Haussmann, S. Simonis, H. Nirschl, and M. Krause, "Direct numerical simulation of decaying homogeneous iso-tropic turbulence - numerical experiments on stability, consistency and accuracy of distinct lattice Boltzmann methods", International Journal of Modern Physics C, (2019).

[4]. S. Green, “FLUID MECHANICS AND ITS APPLICATIONS”, Springer Science+ Business media, b.v., vol. 30, (1995).

[5]. J. Chambers, (Jan 1, 2003). "Wind Shear". Concept to Reality: Contributions of the Langley Research Center to US Civil Aircraft of the 1990s (PDF). NASA. pp. 185–198.

[6]. P. Kilner, G. Yang, A. Wilkes, R. Mohiaddin, D. Firmin, and M. Yacoub, “Asymmetric redirection of flow through the heart”, Nature 404, (2000).

[7]. J. Yao, T. Lundgren, “Experimental investigation of microbursts”, Experiments in Fluids 21, 17–25 (1996).

[8]. M. Stenhoff, Ball Lightning: An Unsolved Problem in Atmospheric Physics 1st edn, Springer, (1999).

[9]. C. Donnelly, K. Metlov, V. Scagnoli, M. Sicairos, M. Holler, N. Bingham, J. Raabe, L. Heyderman, N. Cooper, and S. Gliga, “Experimental observation of vortex rings in a bulk magnet”, Nature Physics vol. 17, pp. 316–321 (2021).

[10]. A. Azuma and A. Obata, “Induced flow variation of the helicopter rotor operating in the vortex ring state”, J. Aircraft, vol. 5, (1968).

[11]. O. Inoue, Y. Hattori, and K. Akiyama, “Calculations of vortex ring states and autorotation in helicopter rotor flow fields”, American Institute of Aeronautics and Astronautics, Inc., (1997).

[12]. G. Ahlin, and R. Brown, “Wake structure and kinematics in the vortex ring state”, Journal of the American Helicopter Society, vol. 54, (2009).

[13]. P. Basset, C. Chen, J. Prasad, and S. Onera, “Prediction of vortex ring state boundary of a helicopter in descending flight by simulation”, Journal of the American Helicopter Society, vol. 53, (2008).

[14]. Morteza Gharib, Edmond Rambod, and Karim Shariff, “A universal time scale for vortex ring formation”, J. Fluid Mech. (1998), vol. 360, pp. 121-140.

[15]. J. Cater, J. Soria, and T. Lim, “The interaction of the piston vortex with a piston-generated vortex ring”, J. Fluid Mech., vol. 499, pp. 327–343, (2004).

[16]. J. Wilson, “Vortex rings generated by a shrouded Hartmann-Sprenger tube”, AIAA journal, vol. 44, (2006).

[17]. R. Mariani, MK. Quinn, and K. Kontis, “A note on the generation of a compressible vortex rings using helium as driver gas”, Journal of Aerospace Engineering, 227(10) 1637–1645, (2013).

[18]. W. Rogers, “On the formation of rotating rings by air and liquids under certain conditions of discharges”, Am. J. Arts., vol.26, pp. 246-258, (1858).

[19]. H. Helmholtz, “Über Integrale der hydrodynamischen Gleichungen, welche den Wirbelbewegungen entsprechen", Journal für die reine und angewandte Mathematik. 55: 25–55, (1858).

[20]. A. Buzukov, “Properties of the formation and motion of vortex rings in water”, Journal of Applied Mechanics and technical Physics, vol. 12, (1971).

[21]. V. Boyarintsev, A. Leont'ev, S. Ya. Sekerzh-Zen'kovlch, and V. I. Sysoev, “Propagation of vortex rings in stratified fluids”, translated from Zhurnal Prikladnoi Mekhaniki i Tekhnicheskoi Fiziki, No.2, pp. 22-26, (1982).

[22]. L. Pismen, and A. Nepomnyashchy, “Stability of vortex rings in a model of superflow”, Physica D, vol. 69, pp. 163-171, (1993).

[23]. P. Orlandi and R. Verzicco, “Vortex rings impinging on walls: axisymmetric and three-dimensional simulations”, J. Fluid Mech., vol. 256, pp. 615-646, (1993).

[24]. S. Tamano, M. Itoh, A. Takagi, and K. Yokota, “Flow visualization of ring vortex in confined swirling flow of polymer solutions due to partially rotating disc”, The Japan society of Mechanical Engineers, No. 09, (2010).

[25]. W. Abdel Kareem, “Tracking of vortical structures in three dimensional decaying homogenous isotropic turbulence”, International journal of modern Physics C, vol.22, pp. 1373-1391, (2011).

[26]. T. Murugan, and S. De, “Numerical visualization of counter rotating vortex ring formation ahead of shock tube generated vortex ring”, Journal of Visualization, 15 (2). pp. 97-100, (2012).

[27]. E. Aydemir, N. Worth, and J. Dawson, “The formation of vortex ring in a strongly forced round jet”, Exp. Fluids 52:729–742, (2012).

[28]. N. Imamura, and K. Matsuuchi, “Relationship between vortex ring in tail fin wake and propulsive force”, Exp. Fluids 54:1605, (2013).

[29]. J. Peng, “Simulation of vortex ring formation and the effect of piston velocity”, Fluid Mechanics: Open Access, vol.2, (2015).

[30]. A. Tinaikar1, S. Advaith and S. Basu, “Understanding evolution of vortex rings in viscous fluids”, J. Fluid Mech., vol. 836, pp. 873-909, (2018).

[31]. O. Bentata, D. Anne-Archard, and P. Brancher, “Experimental studies of low inertia vortex rings in shear thinning fluids”, Physics of Fluids, vol. 30, (2018).

[32]. D. Rebah, “Steady vortex rings in a uniform flow and rearrangements of a function”, Springer Nature Switzerland, vol. 75, (2020).

[33]. K. Yeo, J. Koh, J. Long, and T. New, “Flow transitions in collisions between vortex-rings and density interfaces”, Journal of visualization, vol. 23, pp. 783–791, (2020).

[34]. H. Yu, S. Girimaji, and L. Luo, "DNS and LES of decay-ing isotropic turbulence with and without frame rotation us-ing lattice Boltzmann method", Journal of Computational Physics 209, pp. 599-616, (2005).

[35]. W. Abdel Kareem, Seiichiro Izawa, A K. Xiong, and Y. Fukunishi, “Identification of multi-scale coherent eddy structures in a homogeneous isotropic turbulence”, Progress in Computational Fluid Dynamics, an International Journal, vol.6, (2006).

[36]. W. Abdel Kareem, “A vortex identification method based on strain and enstrophy production invariants”, Int. J. Mod. Phys. C 31, 2050003 (2020).

[37]. T. Chen, X. Wen, J. Wang, Z. Guo, and S. Chen, "Simulation of three-dimensional compressible decaying isotropic turbulence using a redesigned discrete unified gas kinetic scheme", Physics of Fluids 32, (2020).

[38]. L. p. Wang, S. Chen, J.G. Brasseur, and J.C. Wyngaard, “Examination of hypotheses in the Kolmogorov refined turbulence theory through high-resolution simulations”, part 1. Velocity field. J. Fluid Mech., 309:113, 1996.

[39]. K. R. Sreenivasan. On the scaling of the turbulence dissipation rate. Phys. Fluids, 27:1048,1984.

[40]. W. J. T. Bos, L. Shao, and J.-P. Bertoglio. Spectral imbalance and the normalized dissipation rate of turbulence. Phys. Fluids, 19:45101, 2007.